




Cite this: *Toxicol. Res.*, 2018, 7, 923

## Evaluation of the antioxidant, antibacterial and anticancer (lung cancer cell line A549) activity of *Punica granatum* mediated silver nanoparticles

Annu,<sup>a</sup> Shakeel Ahmed,<sup>a,b</sup> Gurpreet Kaur,<sup>c,d</sup> Praveen Sharma,<sup>c</sup> Sandeep Singh<sup>c</sup> and Saiqa Ikram \*<sup>a</sup>

This work aimed to synthesize silver nanoparticles *via* an environmentally benign route, using the aqueous extract of *Punica granatum* as a precursor as well as a stabilizing and reducing agent. The as-synthesized silver nanoparticles were confirmed using UV-visible spectroscopy with an absorbance peak at 450 nm and were thereafter further confirmed using dynamic light scattering (DLS), High Resolution Transmission Electron Microscopy (HR-TEM) and X-Ray Diffraction (XRD). TEM analysis revealed 6–45 nm and spherically dispersed nanoparticles and XRD showed the crystalline nature of the nanoparticles. The free radical scavenging activity of the nanoparticles for DPPH and intracellular reactive oxidative species (ROS) production were observed using dihydroethidium (DHE) non-fluorescent stain and a CellROX® Deep Red fluorescent probe. Antibacterial assays against the most common Gram negative (*Escherichia coli*) and Gram positive (*Staphylococcus aureus*) bacteria showed a higher zone of inhibition against *S. aureus*. Furthermore, the anti-cancerous activity of the biologically synthesized silver nanoparticles was revealed by the inhibited cell growth of lung cancer A549 cells and no cytotoxicity was observed. This may be due to their ability to arrest the cell cycle at G1 phase. Thus, this work provides a gateway to explore more about the anticancer properties of biogenically synthesized silver nanoparticles and these biologically prepared silver nanoparticles have the potential to be utilized in biomedical science.

Received 6th April 2018,  
Accepted 16th May 2018  
DOI: 10.1039/c8tx00103k  
rsc.li/toxicology-research

### 1. Introduction

Plants always play a key role as troubleshooters for tackling environmental problems. With respect to this, it has been observed over the last decade that researchers and scientists have taken a keen interest in plant-derived materials, especially in the developing nanosciences.<sup>1</sup> Nanotechnology is an extremely exploited field of research which includes novel methods of nanoparticle fabrication and their potential applications in various fields. Basically, nanoparticles are known to have clusters of atoms with sizes ranging from 1–100 nm and significantly enhanced physical, chemical and biological pro-

erties compared to those of their macro-scaled counterparts. Nowadays, various applications of metallic nanoparticles are largely dependent upon their shape and controlled size due to their high surface to volume ratio.<sup>2</sup> Nanoparticles are not confined to use in technology based systems such as electronics,<sup>3</sup> sensors,<sup>4</sup> optics,<sup>5</sup> electro-optics, water treatment<sup>6</sup> and space industries, and are instead finding applaudable applications in biomedical fields such as antimicrobials,<sup>7</sup> drug delivery,<sup>8</sup> biomolecular detection and diagnostics,<sup>8</sup> tissue engineering,<sup>9</sup> therapeutics,<sup>10</sup> theranostics<sup>11</sup> and bioimaging.<sup>12</sup>

Among different noble metal nanoparticles such as gold<sup>13</sup> and silver, silver has been put forth for biomedical applications. However, its toxicity towards humans and bodies of water has already been revealed by several researchers with respect to silver ions, which are highly toxic to human cells.<sup>14</sup> On the other hand, the toxicity of biologically synthesized nanoparticles is considered to be less than that of conventionally synthesized nanoparticles, which involve toxic and harsh chemicals and the by-products released are also toxic. Additionally, with the prevalence and enhanced antibiotic resistance of microbes, silver nanoparticles can play a beneficial role because they also exhibit good antimicrobial activity. The

<sup>a</sup>Bio/Polymers Research Laboratory, Department of Chemistry, Jamia Millia Islamia, New Delhi-110025, India. E-mail: sikram@jmi.ac.in;  
Tel: +91-11-26981717(extn-3252)

<sup>b</sup>Department of Chemistry, Government Degree College Mendhar, Jammu and Kashmir-185111, India

<sup>c</sup>Centre for Environmental Science and Technology, Central University of Punjab, Bathinda-151001, India

<sup>d</sup>Laboratory of Molecular Medicine, Centre for Human Genetics and Molecular Medicine, Central University of Punjab, Bathinda-151001, India

procedure for a one-pot green method for the fabrication of silver nanoparticles would be not only environmentally benign but cost-effective too, which is why a green method is a wise route which also avoids the adverse effects of conventional methods. A huge amount of data is available about green routes for the synthesis of silver nanoparticles using plants and plant extracts, including leaf extracts such as *Terminalia arjuna*,<sup>15</sup> *Withania somnifera*,<sup>7</sup> *Coriandrum sativum*<sup>16</sup> and *Crotolaria retusa*,<sup>17</sup> root extracts such as *Diospyros paniculata*,<sup>18</sup> flower extracts such as *Cassia auriculata*,<sup>19</sup> fruit extracts such as *Tamarindus indica*<sup>20</sup> and *Citrullus lanatus*,<sup>21</sup> fruit peel extracts such as *Citrus sinensis*, *Citrus limetta* and *Citrus limon*,<sup>22</sup> seeds and seed oil extracts such as *Dimocarpus longan*,<sup>23</sup> pod husk extracts<sup>24</sup> and paper wasp nests<sup>25</sup> as well. Additionally, bacteria such as *Bacillus safensis* LAU 13 have been utilized in the synthesis of silver nanoparticles.<sup>26,27</sup> In all of these cases, the biochemicals present in the extracts act as capping or stabilizing agents.

Cancer or tumors are one of the leading causes of death worldwide due to severe complications in the body. Since conventional treatments, such as chemotherapy, laser therapy and surgery, can damage tumor cells as well as some normal healthy cells, are expensive and lead to side effects, such as hair loss, fatigue, bone marrow problems, emesis and nausea, it is necessary to develop cost effective, novel and efficient methods for treatment. Silver nanoparticles are quite often utilized by many researchers to treat different types of cancerous cell, due to their unique remarkable properties including antibacterial, antiviral, anti-platelet, anti-tumor and anti-angiogenesis.<sup>28</sup> Durai *et al.* studied the apoptotic effect of silver nanoparticles on the colon cancer HT29 cell line<sup>28</sup> and Nayak *et al.* and Jacob *et al.* revealed the cytotoxic effect and anticancer activity of green synthesized silver nanoparticles on the breast cancer MCF-7 cell line, respectively.<sup>29,30</sup> Similarly, Sukirtha *et al.* observed the cytotoxic effect of silver nanoparticles on HeLa cervical cancer cells and Sriram *et al.* revealed from his *in vitro* and *in vivo* studies that silver nanoparticles significantly increased the survival time for tumor mouse models by about 50% in comparison with tumor controls and therefore they exhibit good antitumor and anti-angiogenic effects. However, neither the inherent biochemical mechanism nor the toxicity mechanism of silver ions or silver nanoparticles have been justified yet.<sup>31</sup> Besides, other nanoparticles such as copper nanoparticles have also been explored for a prostate cancer cell line.<sup>32</sup>

This article reports on the efficacy of biogenically synthesized silver nanoparticles using the fruit waste (peel) aqueous extract of *Punica granatum* towards antimicrobial activity against *E. coli* and *S. aureus*, antioxidant activity with DPPH and ROS production using dihydroethidium (DHE) non-fluorescent stain and CellROX® Deep Red fluorescent probe, cell viability and anticancer activity against the lung cancer cell line A549. Moreover, the combined effect of silver nanoparticles and doxorubicin drug was also observed against the cancerous cell line A549.

## 2. Experimental section

### 2.1 Materials and methods

Fresh pomegranates were procured from a local market in New Delhi, India. Silver nitrate was purchased from Merck Chemicals (Mumbai, India) and was used as purchased without any further purification. All of the glassware was washed thoroughly with chromic acid, then with double distilled water and then transferred to an oven for drying before being ready to use. Chemicals, including DMSO solution, dihydroethidium (DHE), butylhydroxytoluene (BHT) and doxorubicin drug, were all purchased from Sigma-Aldrich and used without further purification. Fresh blood (around 5 mL) was drawn from healthy individuals as per protocol number CUPB/cc/14/IEC/4483, Government of India. For blood cells, RPMI-1640 media with 5% fetal calf serum (FCS), RBC lysis buffer (1×) and CellROX® Deep Red from Invitrogen was used. MacConkey broth and MacConkey Agar were purchased from HiMedia, Mumbai. All of the cell lines were acquired from the National Cell Repository, NCCS, Pune, India. For the lung cancer cell line A549, DMEM media augmented with 10% fetal bovine serum (FBS) and 1× antibiotic solution with 1% Pentsrip (50 U mL<sup>-1</sup> penicillin G, 50 Ig mL<sup>-1</sup> streptomycin sulfate and 1.25 lg mL<sup>-1</sup> amphotericin B) was obtained from Invitrogen.

### 2.2. Preparation of the plant extract

Initially, *Punica granatum* was peeled and washed twice with distilled water, then with double distilled water to remove dust particles and debris. The peel was dried and weighed about 10 g. Then, it was poured into a 250 mL round bottom flask containing doubled distilled water and heated at 50 °C for 30 min. The peel extract thus obtained was filtered using Whatman no. 1 filter paper to remove solid particles and the filtrate was stored at a low temperature of about 4 °C in a glass media bottle for further experimental usage.

### 2.3. Synthesis of the AgNPs

Silver nitrate aqueous solution (4 mM) was prepared in a 250 mL Erlenmeyer flask. To 10 mL of AgNO<sub>3</sub>, 1 mL of *Punica granatum* peel extract was added to the aqueous solution in a dark chamber, in order to reduce the photoactivation of the AgNO<sub>3</sub> aqueous solution. A colour change was observed and UV-vis spectra were recorded thereafter. The colour of the solution changed from colourless to light yellow and further to a brownish colour, which somewhat confirms the formation of silver nanoparticles. Further characterisation was performed using various advanced techniques to determine the size and shape of the synthesised nanoparticles.

### 2.4. Characterisation techniques

Different characterisation techniques were utilised in order to confirm the formation of silver nanoparticles. UV-vis spectra were obtained using a Shimadzu (UV-1800, Japan) UV-Visible spectrophotometer at room temperature with 1 nm resolution from 300 nm to 700 nm for maximum absorption. Dynamic

Light Scattering (DLS) was carried out using a DLS spectrometer 201 to determine the size of the synthesised nanoparticles. TEM images were obtained using a 300 kV HRTEM TECHNAI G2 30S TWIN operated at 3000 kV accelerated voltage. X-ray diffraction using a Rigaku Ultima IV was used to characterize the size of the silver nanoparticles.

## 2.5. Antioxidant activity of the nanoparticles

The DPPH free radical scavenging activity was evaluated using the method reported by Marinova *et al.* with a few modifications.<sup>33</sup> Three hundred microliters of 200  $\mu\text{M}$  DPPH (in methanol) was added to one hundred microliters of S4 (10  $\mu\text{g ml}^{-1}$ ), E4 (10  $\mu\text{g ml}^{-1}$ ) and BHT (50  $\text{mg ml}^{-1}$  or 100  $\text{mg ml}^{-1}$ ), using the given concentrations as standard. Then, the mixture was incubated in the dark for 30 min after mixing. The absorbance at 517 nm was measured against a blank (methanol). The scavenging of free radicals was determined using the following formula:

$$\% \text{ Scavenging} = \frac{\text{Absorbance control} - \text{Absorbance of Test Sample}}{\text{Absorbance of Sample}} \times 100$$

**2.5.1. Intracellular ROS production using DHE staining.** In order to evaluate intracellular reactive oxygen species, DHE stain (non-fluorescent) was used to evaluate the intracellular ROS levels in A549 cells, seeded in 96-well plates at  $1.0\text{--}1.2 \times 10^4$  cells per well.  $\text{H}_2\text{O}_2$  treatment was used as a positive control. The cultured cells were treated with S4 (5, 10  $\mu\text{g ml}^{-1}$ ) and E4 (10  $\mu\text{g ml}^{-1}$ ) for 48 h. Then, DHE solution was added and incubated for 30 min in the absence of light, which becomes fluorescent upon superoxide oxidation. Fluorescence with an excitation wavelength of 518 nm and emission wavelength of 605 nm was measured using a microplate reader.

**2.5.2. Intracellular ROS production using CellROX® Deep Red staining.** The generation of intracellular ROS was detected using the CellROX® Deep Red fluorescent probe (Invitrogen). The cells were treated with S4 and E4 (10  $\mu\text{g ml}^{-1}$ ) for 24 h and exposed to CellROX® Deep Red (5  $\mu\text{M}$ , 30 min) at 37 °C under 5%  $\text{CO}_2$  atmosphere in the dark. Then, the fluorescence was measured at an excitation wavelength of 633 nm and an emission of 665 nm.

## 2.6. Antimicrobial assay

Antimicrobial experiments were performed against Gram negative (*Escherichia coli*) and Gram positive (*Staphylococcus aureus*) bacteria through an agar well diffusion method. Firstly, a nutrient medium, MacConkey broth (purchased from HiMedia), was prepared to subculture the bacteria. The bacteria were grown after overnight incubation at 37 °C for 24 hours. All of the equipment was first autoclaved for sterilization and then used for further experimental procedures. 5 mm diameter holes were made in the agar plates and saturated with *P. granatum* peel aqueous extract, AgNPs and double distilled water as a control. After that, bacteria was spread across the agar plates and they were then sealed with paraffin

wax. These agar plates were then again incubated at 37 °C for 24 hours. The zones of inhibition around the peel extract and silver nanoparticles were observed and reported.

## 2.7. Cytotoxicity and anticancer activity

The non-toxic doses of silver nanoparticles S4 and E4 were selected based on preliminary cytotoxic studies (MTT assay). Cell cycle analysis was conducted to explore the potential of the biologically synthesized silver nanoparticles acting inside the cell. Cell toxicity was evaluated using an MTT assay. Human peripheral blood mononucleated cells (hPBMC) were seeded in 96-well culture plates and maintained in a RPMI-1640 medium supplemented with 5% fetal calf serum and antibiotics. The cells were treated with six different concentrations of S4 (0.5, 1, 5, 10 and 50  $\mu\text{g ml}^{-1}$ ) and non-treated cells were used as the control. Cell viability was evaluated under three time periods *i.e.* 24 h, 48 h and 72 h at 37 °C with 5%  $\text{CO}_2$ . Then, 20  $\mu\text{L}$  of MTT solution (5  $\text{mg mL}^{-1}$ ) was added to each well and incubated for 3 h in the dark at 37 °C. 100  $\mu\text{L}$  of DMSO was added and incubated for 30 min. The resultant formazan formed by viable cells was measured using a multi-mode plate reader at 570 nm wavelength.

## 2.8. Cell cycle analysis

Cells were treated with S4 and E4 (10  $\mu\text{g ml}^{-1}$ ) for 24 h for cell cycle analysis and uniformly fixed in ethanol for staining. About 200  $\mu\text{L}$  of ethanol-fixed cells were processed according to the Muse cell cycle analysis kit. Then, the cell suspension samples were transferred to microcentrifuge tubes prior to analysis using a Muse™ Cell Analyzer.

# 3. Results and discussion

## 3.1. Visual observations

Upon adding 1 mL of extract to 10 mL of 4 mM  $\text{AgNO}_3$  solution, there was a colour change in the solution from yellowish to dark brown after 15 minutes of incubation time (Fig. 1). This colour change inferred the formation of silver nanoparticles because it was due to the excitation of surface plasmon vibrations. When the electrons of a conduction band oscillate or vibrate collectively in resonance then a unique optical property is exhibited, known as surface plasmon resonance.

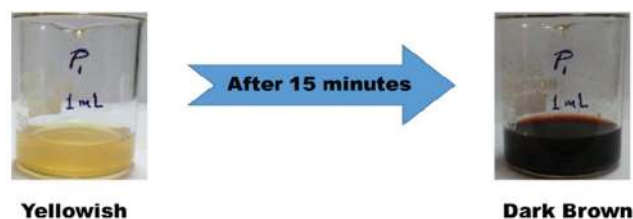


Fig. 1 Visual representation of the formation of silver nanoparticles.

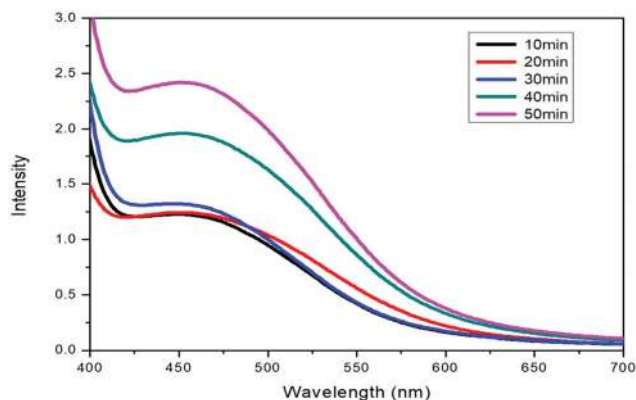


Fig. 2 UV-vis spectral representation of silver nanoparticles.

### 3.2. UV-visible spectroscopy

Upon the addition of 1 mL of extract to 10 mL of  $\text{AgNO}_3$  solution, the colour of the solution changed to reddish dark brown, indicating the formation of nanoparticles. This was further confirmed by UV-visible spectroscopy. The plasma resonance band of the UV-visible spectra was observed in the range of 440–460 nm (Fig. 2). There is an increase in the intensity of the band on increasing the time interval, indicating the formation of more nanoparticles with time and colour intensity also increases with increasing incubation time. The results are very close to those already reported in the literature.<sup>34</sup>

### 3.3. Dynamic light scattering

The DLS histograms of the synthesized silver nanoparticles show two peaks at around 11 nm and 49 nm, as depicted in Fig. 3. The studies based on DLS revealed that the average size of the biogenically synthesized silver nanoparticles was observed at around 10–50 nm. This was due to large water

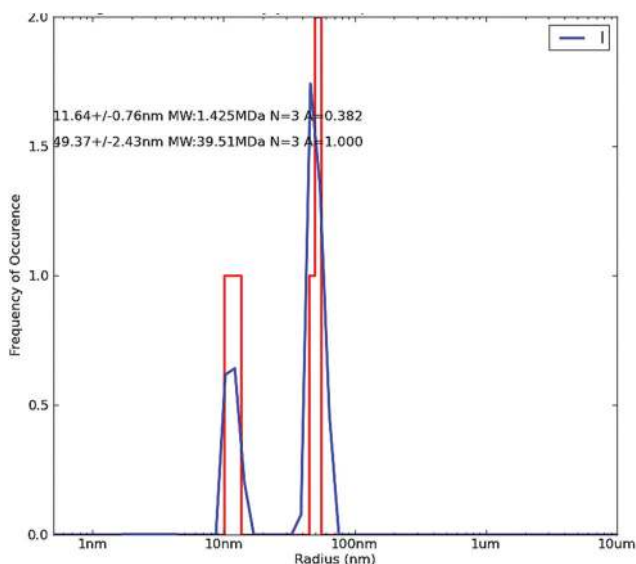


Fig. 3 Dynamic light scattering (DLS) of silver nanoparticles.

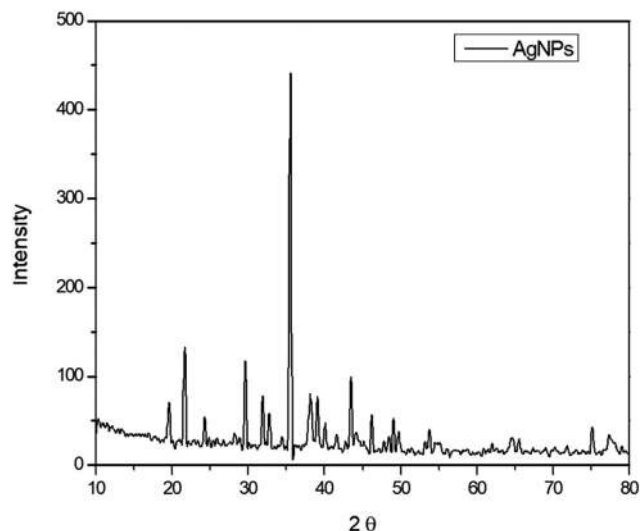


Fig. 4 X-ray diffraction pattern of silver nanoparticles.

molecules present in the solution with hydrogen bonding, leading to increments in the hydrodynamic radius of the nanoparticles.

### 3.4. X-ray diffraction

The XRD patterns show the distinctive diffraction peaks of silver nanoparticles at  $2\theta = 35.53, 38.20, 43.52, 64.49$  and  $77.29$  (Fig. 4). A strong diffraction peak was ascribed to the silver nanoparticles with plant extract. The XRD pattern thus clearly indicated that the synthesized silver nanoparticles were crystalline in nature. Due to the crystallization of the bioorganic phases of the rind extract over silver nanoparticles, some small peaks were also observed. The results are in good agreement with those found in the literature.<sup>35</sup>

### 3.5. High resolution transmission electron microscopy

HR-TEM was used to confirm the formation, shape and size of the biogenically synthesized silver nanoparticles and it was found that these biologically synthesized silver nanoparticles were universally dispersed, spherical in shape and around 6–45 nm in size (Fig. 5).

### 3.6. The antioxidant activity and intracellular ROS scavenging activity of AgNPs

The free radical scavenging capacity of the nanoparticles was determined using a DPPH free radical scavenging assay. DPPH tests demonstrated that these nanoparticle were good free radical scavengers, as depicted in Fig. 6. The results showed that the nanoparticles at  $10 \mu\text{g ml}^{-1}$  concentration achieved 100% scavenging activity compared to BHT at concentrations of 50 and  $100 \mu\text{g ml}^{-1}$  as reference compounds. Therefore, these nanoparticles exhibit the potential to combat free radicals generated as a result of oxidative stress. In this context, it was further planned to monitor antioxidant activity *in vitro* by



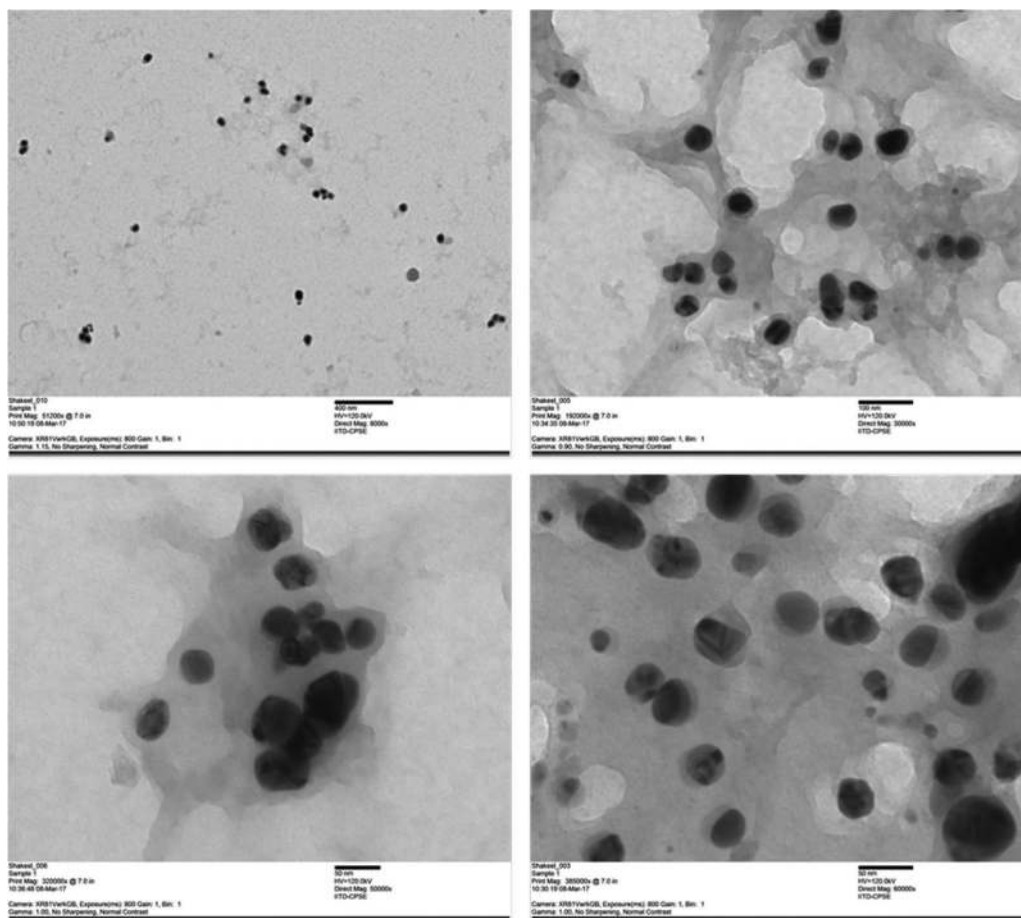


Fig. 5 TEM images of biogenically synthesized silver nanoparticles.

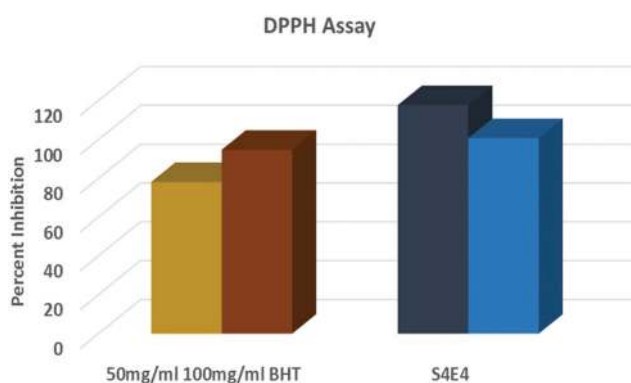


Fig. 6 The antioxidant activity of the S4 AgNPs and the extract using a DPPH assay.

inducing oxidative stress using  $H_2O_2$  and pesticides in the upcoming sections.

Intracellular ROS scavenging was measured using CellROX® Deep Red and a DHE assay *via* inducing oxidative stress using  $H_2O_2$  and pesticides. Cells were treated with nanoparticles as well as  $H_2O_2$  pretreatment (30  $\mu M$  for one hour)

followed by nanoparticles at different concentrations: S1 (0.5  $\mu g mL^{-1}$ ) and S2 (10  $\mu g mL^{-1}$ ) and extract E1 (1  $\mu L$ ) and E2 (10  $\mu L$ ) treatment for 24 h. The next day, the treated cells were exposed to DHE in the absence of light to evaluate intracellular ROS in the cells in response to the nanoparticles. Non-fluorescent DHE easily permeates cell membranes that get oxidized by  $O_2^-$  and converted to ethidium bromide (fluorescent) and intercalates into nuclear DNA.

The  $H_2O_2$  treatment resulted in a significant increase in fluorescence intensity, indicating higher intracellular free radical production inside the cell (Fig. 7a). In contrast, the nanoparticles at both concentrations (S1 and S2) demonstrated less intensity than the control, indicating that the treatment resulted in decreased ROS production. Interestingly, fluorescence intensity decreased in the cells treated with  $H_2O_2$  followed with treatment by nanoparticles, indicating that the nanoparticles have the potential to quench the induced reactive oxygen species. Similarly, free radical scavenging activity was evaluated in response to oxidative stress induced using pesticide exposure and  $H_2O_2$  (Fig. 7b). The nanoparticle treatment scavenges free radicals produced as a result of pesticides that enter the food chain, as reported by many researchers. Intracellular ROS generation using the fluorescent probe

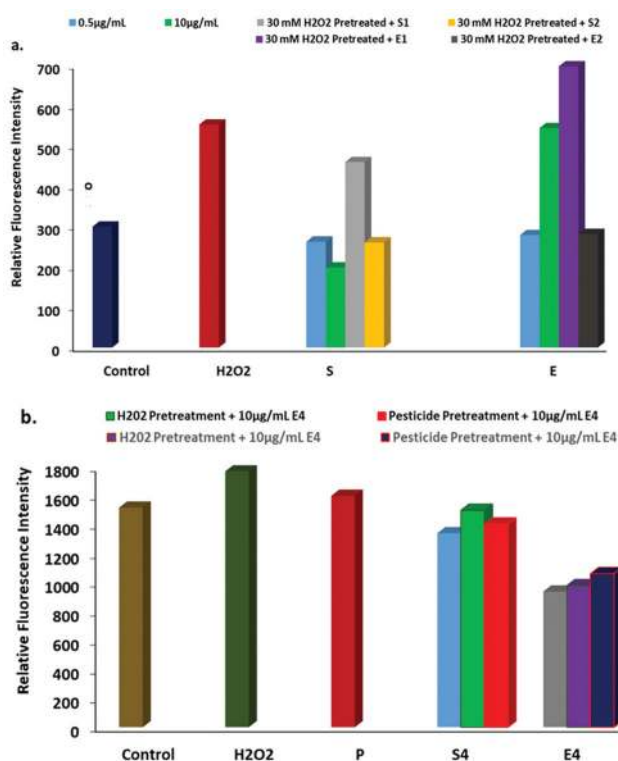


Fig. 7 Intracellular ROS generation. a. The effect of the AgNPs and the extract on H<sub>2</sub>O<sub>2</sub> induced free radical production using a DHE assay and b. the effect of the AgNPs and the extract on H<sub>2</sub>O<sub>2</sub> and pesticide induced free radical production using the fluorescent probe CellROX® Deep Red.

CellROX® Deep Red revealed similar results to the DHE assay. The nanoparticle treatment resulted in decreased oxidative stress induced due to H<sub>2</sub>O<sub>2</sub> as well as pesticide treatment in the cells (Fig. 7a and b).

### 3.7. Antimicrobial activity

The results of the antimicrobial activity of the biologically synthesized nanoparticles are shown in Table 1. Good antimicrobial activity is shown against *E. coli* in comparison to *S. aureus*, which might be due to interactions between nanoparticles and different microorganisms. The mechanism of the antimicrobial activity of the nanoparticles probably involves the attachment of particles to the cell walls of the microorganisms, where they disrupt the plasma membrane. Studies also

Table 1 Zones of inhibition (in mm) of silver nanoparticles against *E. coli* and *S. aureus* bacteria

Components	Zone of inhibition (mm)	
	<i>E. coli</i>	<i>S. aureus</i>
Control	N/A	N/A
Plant extract	N/A	N/A
Silver nitrate	9.3	11.0
Silver nanoparticles	15.5	16.5

confirm that silver nanoparticles and silver ions invade bacterial walls and inhibit many enzymes, leading to protein inhibition and death.

### 3.8 Cytotoxicity of the green synthesized AgNPs with anti-cancer properties

Cell viability was evaluated using an MTT [3-(4,5-dimethylthiazolyl)-2,5-diphenyl-tetrazolium bromide] assay, *i.e.* based on the reduction of MTT by mitochondrial dehydrogenase to purple formazan in living cells, reflecting the functioning of mitochondria in viable cells, allowing for the measurement of cell viability and cytotoxicity.

The cytotoxicity of the silver nanoparticles was evaluated *in vitro* in hPBMC at different concentrations (0.5, 1, 5, 10 and 50 μg ml<sup>-1</sup>). The cytotoxicity analysis of the sample shows no cytotoxicity in the nanoparticles at any selected dose (Fig. 8a) in normal cells, whereas they inhibited the cell growth of A549 cells (Fig. 8b). The results of cell viability studies in hPBMC suggest that the cells are growing in a healthier environment as the cell viability increased after AgNP treatment. On the other hand, in non-small lung cancer cell lines there was 50% inhibition in the cell growth at 5 μg ml<sup>-1</sup> after 48 and 72 h. It suggests that the silver nanoparticles are non-toxic for normal body cells, but cytotoxic for cancer cells only. This is one of the major challenges in cancer therapeutics as research on cancer cell target based medication is lacking. It can be pro-

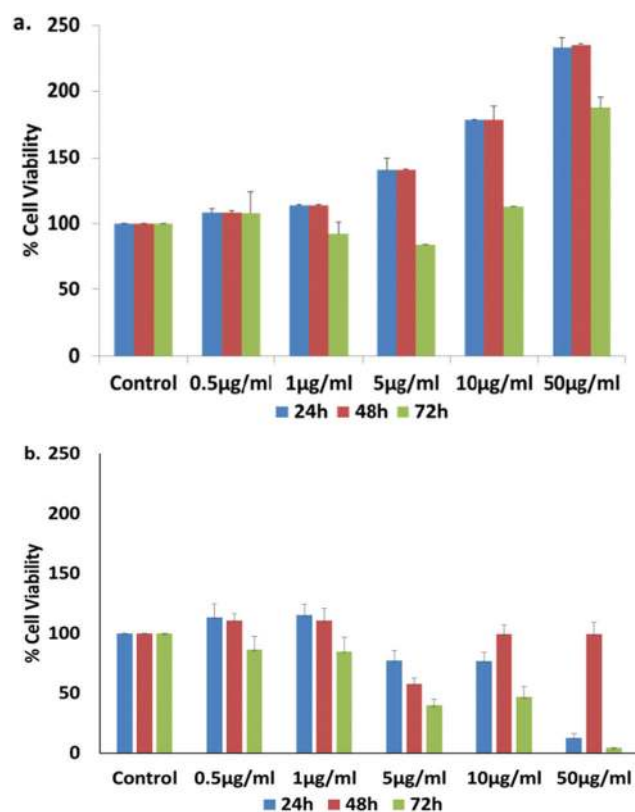
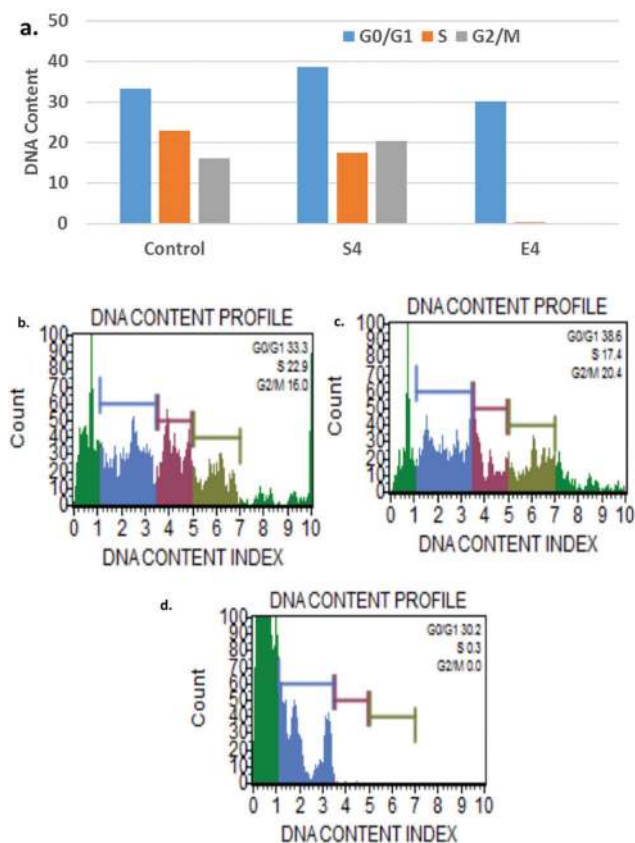


Fig. 8 Cell viability percentage upon treatment with S4 green AgNPs on (a) hPBMC and (b) A549 lung cancer cell lines at 24, 48 and 72 h.

posed that these nanoparticles exhibit anti-cancerous properties for lung cancer without affecting the normal cells of the body. Cell proliferation has been monitored at higher concentrations (10 and 50  $\mu\text{g ml}^{-1}$ ) in normal cells, which may be due to the higher antioxidant activity of nanoparticles, evaluated in the upcoming sections.

### 3.9 Cell cycle analysis

Our previous results imply cancer cell specific cytotoxicity by the nanoparticles and therefore we further explored the effect of AgNPs on the cell cycle. The nanoparticles effect on cell cycle progression was demonstrated in A549 cells. The Muse histogram displayed peaks at G0/G1 (33.3%), G2/M (16%) and S (22.9%) phases for control. In contrast, the nanoparticle treatment results show increases in the peak values of G0/G1 and G2/M with increases of 15.92% and 27.5%, respectively (Fig. 9). The extract resulted in the complete loss of S and G2/M phases indicating apoptosis at G1 phase. The arrest at the G2/M checkpoint decides survival with DNA damage that may activate either repair or apoptosis-like programs and the G2/M checkpoint is reported to be a major target for DOX-based chemotherapy. Therefore, combined therapy could also improve the chemotherapeutic efficacy of doxorubicin drugs.



**Fig. 9** a. The effect of AgNPs and the extract on the cell cycle progression with respect to control treatment, b. the DNA content profile of the control, c. the DNA content profile of the AgNPs and d. the DNA content profile of the extract.

These results demonstrate a change in cell cycle dynamics in response to silver nanoparticle and extract treatment.

## 4. Conclusions

This study presents a green, eco-friendly, cost-effective route for the synthesis of stable colloidal silver nanoparticles using pomegranate fruit waste (peel extract). The results show the formation of silver nanoparticles within a short duration at room temperature, without the involvement of any hazardous chemicals or energy use. The synthesised green silver nanoparticles showed good antimicrobial activity against both Gram positive and Gram negative bacteria. The AgNPs were very potently anti-oxidant with the ability to quench induced free radicals from cells, and are therefore effective in protecting cells from various environmental toxins. In addition, the data suggests no cytotoxicity of the nanoparticles at any selected doses in normal cells (hPBMC), whereas the nanoparticles inhibited the cell growth of A549 cells. This may be due to their ability to arrest the cell cycle at G1 phase or need further research. It can be proposed that these nanoparticles exhibit anti-cancerous properties for lung cancer and this may indicate a new direction to explore their potential as anticancer therapy.

## Ethical statement

Human peripheral blood monocytes were collected from a volunteer after proper approval from the Institute Ethical Committee of Central University of Punjab (CUPB). Informed consent of the volunteer was obtained and all of the guidelines regarding sample usage as well as proper biological waste disposal protocols as per CUPB regulations were followed.

## Conflicts of interest

There are no conflicts of interest.

## Acknowledgements

Annu appreciatively acknowledges the University Grant Commission (UGC), New Delhi, India for the financial support. GK is the recipient of the Maulana Azad National Fellowship. PS and SS are thankful to DST for SERB extra mural project (SR/SO/AS-31/2014).

## References

- 1 N. H. Rao, N. Lakshmi, S. V. Pammi, P. Kollu, S. Ganapaty and P. Lakshmi, *Mater. Sci. Eng., C*, 2016, **62**, 553–557.
- 2 K. M. M. Abou El-Nour, A. Eftaiha, A. Al-Warthan and R. A. A. Ammar, *Arabian J. Chem.*, 2010, **3**, 135–140.
- 3 S. Ummartyotin, N. Bunnak, J. Juntaro, M. Sain and H. Manuspiya, *C. R. Chim.*, 2012, **15**, 539–544.

- 4 M. R. Bindhu and M. Umadevi, *Spectrochim. Acta, Part A*, 2014, **128**, 37–45.
- 5 D. D. Evanoff and G. Chumanov, *ChemPhysChem*, 2005, **6**, 1221–1231.
- 6 S. Kanchi, *J. Environ. Anal. Chem.*, 2014, **1**, 10–12.
- 7 S. Ahmed, Annu, I. Zafeer and S. Ikram, *J. Bionanosci.*, 2016, **10**, 1–7.
- 8 F. Benyettou, R. Rezgui, F. Ravaux, T. Jaber, K. Blumer, M. Jouiad, L. Motte, J.-C. Olsen, C. Platas-Iglesias, M. Magzoub and A. Trabolsi, *J. Mater. Chem. B*, 2015, **3**, 7237–7245.
- 9 E. I. Alarcon, K. I. Udekwu, C. W. Noel, L. B.-P. Gagnon, P. K. Taylor, B. Vulesevic, M. J. Simpson, S. Gkotzis, M. M. Islam, C.-J. Lee, A. Richter-Dahlfors, T.-F. Mah, E. J. Suuronen, J. C. Scaiano and M. Griffith, *Nanoscale*, 2015, **7**, 18789–18798.
- 10 R. R. Arvizo, S. Bhattacharyya, R. A. Kudgus, K. Giri, R. Bhattacharya and P. Mukherjee, *Chem. Soc. Rev.*, 2012, **41**, 2943–2970.
- 11 P. Di Pietro, G. Strano, L. Zuccarello and C. Satriano, *Curr. Top. Med. Chem.*, 2016, **16**, 3069–3102.
- 12 Y. K. Gun'ko, *Nanomaterials*, 2016, **6**, 105, DOI: 10.3390/nano6060105.
- 13 S. Kanchi, G. Kumar, A. Y. Lo, C. M. Tseng, S. K. Chen, C. Y. Lin and T. S. Chin, *Arabian J. Chem.*, 2018, **11**, 247–255.
- 14 A. Katsumiti, D. Gilliland, I. Arostegui, M. P. Cajaraville, M. Fernández and M. Schuster, *PLoS One*, 2015, **10**, e0129039.
- 15 S. Ahmed and S. Ikram, *J. Nanomed. Nanotechnol.*, 2015, **6**, 4, DOI: 10.4172/2157-7439.1000309.
- 16 P. Sathishkumar, J. Preethi, R. Vijayan, A. R. M. Yusoff, F. Ameen, S. Suresh, R. Balagurunathan and T. Palvannan, *J. Photochem. Photobiol., B*, 2016, **163**, 69–76.
- 17 S. Ahmed, Annu, K. Manzoor and S. Ikram, *J. Bionanosci.*, 2016, **10**, 282–287.
- 18 K. Muthu and S. Priya, *Spectrochim. Acta, Part A*, 2017, **179**, 66–72.
- 19 N. Jayaprakash, J. J. Vijaya, K. Kaviyarasu, K. Kombaiyah, L. J. Kennedy, R. J. Ramalingam, M. A. Munusamy and H. A. Al-Lohedan, *J. Photochem. Photobiol., B*, 2017, **169**, 178–185.
- 20 J. K. Patra, G. Das and K.-H. Baek, *J. Photochem. Photobiol., B*, 2016, **161**, 200–210.
- 21 Annu, S. Ahmed, G. Kaur, P. Sharma, S. Singh and S. Ikram, *J. Appl. Biomed.*, 2018, DOI: 10.1016/j.jab.2018.02.002.
- 22 F. U. Khan, Y. Chen, N. U. Khan, Z. U. H. Khan, A. U. Khan, A. Ahmad, K. Tahir, L. Wang, M. R. Khan and P. Wan, *J. Photochem. Photobiol., B*, 2016, **164**, 344–351.
- 23 A. Lateef, M. A. Azeez, T. B. Asafa, T. A. Yekeen, A. Akinboro, I. C. Oladipo, L. Azeez, S. A. Ojo, E. B. Gueguim-Kana and L. S. Beukes, *J. Nanostruct. Chem.*, 2016, **6**, 159–169.
- 24 A. Lateef, M. A. Akande, S. A. Ojo, B. I. Folarin, E. B. Gueguim-Kana and L. S. Beukes, *3 Biotech*, 2016, **6**.
- 25 A. Lateef, S. A. Ojo and S. M. Oladejo, *Process Biochem.*, 2016, **51**, 1406–1412.
- 26 A. Lateef, S. A. Ojo and J. A. Elegbede, *Nanotechnol. Rev.*, 2016, **5**, 601–622.
- 27 T. V. M. Sreekanth, M. Pandurangan, D. H. Kim and Y. R. Lee, *J. Cluster Sci.*, 2016, **27**, 671–681.
- 28 P. Durai, A. Chinnasamy, B. Gajendran, M. Ramar, S. Pappu, G. Kasivelu and A. Thirunavukkarasu, *Eur. J. Med. Chem.*, 2014, **84**, 90–99.
- 29 D. Nayak, A. P. Minz, S. Ashe, P. R. Rauta, M. Kumari, P. Chopra and B. Nayak, *J. Colloid Interface Sci.*, 2016, **470**, 142–152.
- 30 S. J. P. Jacob, V. L. S. Prasad, S. Sivasankar and P. Muralidharan, *Food Chem. Toxicol.*, 2017, **109**(2), 951–956.
- 31 R. Sukirtha, K. M. Priyanka, J. J. Antony, S. Kamalakkannan, R. Thangam, P. Gunasekaran, M. Krishnan and S. Achiraman, *Process Biochem.*, 2012, **47**, 273–279.
- 32 M. I. Sriram, S. B. M. Kanth, K. Kalishwaralal and S. Gurunathan, *Int. J. Nanomed.*, 2010, **5**, 753–762.
- 33 E. M. Marinova and N. V. Yanishlieva, *Food Chem.*, 1997, **58**, 245–248.
- 34 E. E. Elemike, D. C. Onwudiwe, A. C. Ekennia, R. C. Ehiri and N. J. Nnaji, *Mater. Sci. Eng., C*, 2017, **75**, 980–989.
- 35 A. R. Allafchian, S. Z. Mirahmadi-Zare, S. A. H. Jalali, S. S. Hashemi and M. R. Vahabi, *J. Nanostruct. Chem.*, 2016, **6**, 129–135.